

SIGNIFICANCE AND LIMITATIONS OF STABLE OXYGEN ISOTOPE RATIOS IN THE APATITE PHOSPHATE OF ARCHAEOLOGICAL VERTEBRATE FINDS FOR PROVENANCE ANALYSIS IN AN ALPINE REFERENCE REGION*

M. MAUDER

Ludwig-Maximilians-Universität München, Institut für Informatik, Lehr- und Forschungseinheit für Datenbanksysteme, Oettingenstraße 67 D-80538 Munich, Germany

E. NTOUTSI

Leibniz-Universität Hannover, Appelstr. 4 D-30167 Hannover, Germany

P. KRÖGER

Ludwig-Maximilians-Universität München, Institut für Informatik, Lehr- und Forschungseinheit für Datenbanksysteme, Oettingenstraße 67 D-80538 Munich, Germany

C. MAYR

Friedrich-Alexander Universität Erlangen-Nürnberg, Institut für Geographie, Glückstr. 5 D-91054 Erlangen, Germany

A. TONCALA

Ludwig-Maximilians-Universität München, Biozentrum Martinsried, Grosshaderner Str. 2 D-82152 Martinsried, Germany

S. HÖLZL

RiesKraterMuseum Nördlingen, Eugene-Shoemaker-Platz 1 D-86720 Nördlingen, Germany

and **G. GRUPE†**

Ludwig-Maximilians-Universität München, Biozentrum Martinsried, Grosshaderner Str. 2 D-82152 Martinsried, Germany

A multi-isotope fingerprint consisting of $\delta^{18}O_{\text{phosphate}}$, $^{87}\text{Sr}/^{86}\text{Sr}$, $^{208}\text{Pb}/^{204}\text{Pb}$, $^{207}\text{Pb}/^{204}\text{Pb}$, $^{206}\text{Pb}/^{204}\text{Pb}$, $^{208}\text{Pb}/^{207}\text{Pb}$ and $^{206}\text{Pb}/^{207}\text{Pb}$ was established in the bioapatite of 219 individual archaeofaunal remains (cattle, pig, red deer) excavated from sites located along a specific transect of the European Alps, namely the Inn–Eisack–Adige–Brenner Passage, that has been of eminent importance since European prehistory. This reference area is vertically stratified, and since $\delta^{18}O$ in the skeleton is influenced by climate, water source, physiology and even culture, we tested the relative contribution and importance of $\delta^{18}O$ as a component of the

*Received 28 November 2016; accepted 8 February 2018

†Corresponding author: email g.grupe@lrz.uni-muenchen.de

© 2018 University of Oxford

multi-isotope fingerprint for provenance analysis in this alpine region by a novel mathematical approach. In particular, we adapted a supervised learning approach through expectation–maximization (EM) clustering for fingerprint extraction and evaluated the contribution of each isotopic ratio to the data structure. While an altitude effect was evident in $\delta^{18}\text{O}$, its overall structural importance in the complete isotopic fingerprint was rather low. Therefore, provenance analysis of bioarchaeological finds in this region is possible by measuring stable Sr and Pb ratios alone, which is of considerable importance when $\delta^{18}\text{O}$ values are not available, e.g., in cremated finds, although some information is lost. Whether this is tolerable depends on the scientific question to be solved.

KEYWORDS: BIOAPATITE, PROVENANCE ANALYSIS, EUROPEAN ALPS, STABLE ISOTOPES, DATA-MINING, $\delta^{18}\text{O}$

INTRODUCTION

$\delta^{18}\text{O}_{\text{apatite}}$ in archaeological skeletons is frequently measured for the scope of provenance analysis and/or an assessment of ecogeographical parameters in the past (Lightfoot and O’Connell 2016 and references therein). Since stable oxygen (O) isotopes are bound to hydrological cycles, and since a major part of the oxygen in the bioapatite of a consumer is derived from drinking water and the liquid part of the food, a relation between tissue $\delta^{18}\text{O}$ and the respective isotopic ratio of meteoric water exists (Kohn and Cerling 2002). Species-specific peculiarities with regard to thermoregulation and drinking behaviour need to be taken into account, and also environmental parameters such as the overall humidity (Kohn 1996). Species-specific regressions between $\delta^{18}\text{O}_{\text{phosphate}}$ and $\delta^{18}\text{O}_{\text{meteoric water}}$ have been established experimentally (Longinelli 1984; D’Angela and Longinelli 1990), but recent research emphasizes the uncertainties of such estimates and recommends a direct mapping and comparison of apatite $\delta^{18}\text{O}$ values (Pollard *et al.* 2011; Pellegrini *et al.* 2016). It has also been emphasized that the majority of archaeological provenance studies suffer from a poor definition of local and non-local cut-off values, and high intra-sample variability that might exceed 3‰ in local humans (Lightfoot and O’Connell 2016; Pellegrini *et al.* 2016).

The assessment of the place of origin of non-local finds, be they human or animal, is attempted by use of the known regional variability of $\delta^{18}\text{O}$ in precipitation. Basically, O isotope variations in the hydrological cycle are due to isotope fractionations related to the evaporation of ocean water and subsequent condensation processes during precipitation formation. $\delta^{18}\text{O}$ in precipitation strongly depends on the condensation temperature (Horita and Wesolowski 1994). Therefore, a significant correlation between ambient air temperature and $\delta^{18}\text{O}$ in precipitation exists (Dansgaard 1964; Rozanski *et al.* 1993). This temperature effect averages 0.695‰/°C in Europe (Rozanski *et al.* 1992). Another important control is the history of an air mass determined by the landform configuration and atmospheric circulation patterns, leading to the known continental, latitude and altitude effects (Dansgaard 1964; Gat 1996). With increasing altitude above sea level, $\delta^{18}\text{O}$ in precipitation becomes also depleted because of a decline in temperature and the preferred precipitation of water molecules carrying the heavy isotope as rainfall (Humer *et al.* 1995; Marshall *et al.* 2007).

Isotope records of precipitation are archived at meteorological stations belonging to the Global Network of Isotopes in Precipitation (GNIP; http://www-naweb.iaea.org/napc/ih/IHS_resources_gnip.html). For sites with no nearby hydrological GNIP station, expectation values for $\delta^{18}\text{O}$ in precipitation can be estimated (www.waterisotopes.org). It has to be emphasized, however, that the majority of these expectation values and derived O isotopic maps rely on

interpolations between a finite number of hydrological stations. Contrary to the United States, O isotopic maps for other continents, including Europe, are still unsatisfactory (Ben-David and Flaherty 2012).

In this study, $\delta^{18}\text{O}_{\text{phosphate}}$ and other stable isotopic ratios were measured in archaeological bones of three largely residential vertebrate taxa: pig, cattle and red deer. While cattle and pigs were kept in or at least near to settlements and, therefore, should have been mainly local to the site of recovery, red deer had a larger home range and integrated local isotopic ratios on a higher scale. In general, mammals with a large body size integrate the isotopic composition of meteoric water better than small mammals (Bryant and Froelich 1995), and compact bone integrates any seasonal variability or short-term weather conditions because of its slow turnover rate, contrary to dental enamel which precipitates during juvenile age and is highly influenced by the season of birth. The finds come from sites along a specific transect across the Alps, namely the Inn–Eisack–Adige passage via the Brenner Pass (Fig. 1), which had been in use since the Mesolithic and is, therefore, of eminent archaeological importance. Shortly after the beginning of prehistoric metalworking, the central Alpine regions were sought after because

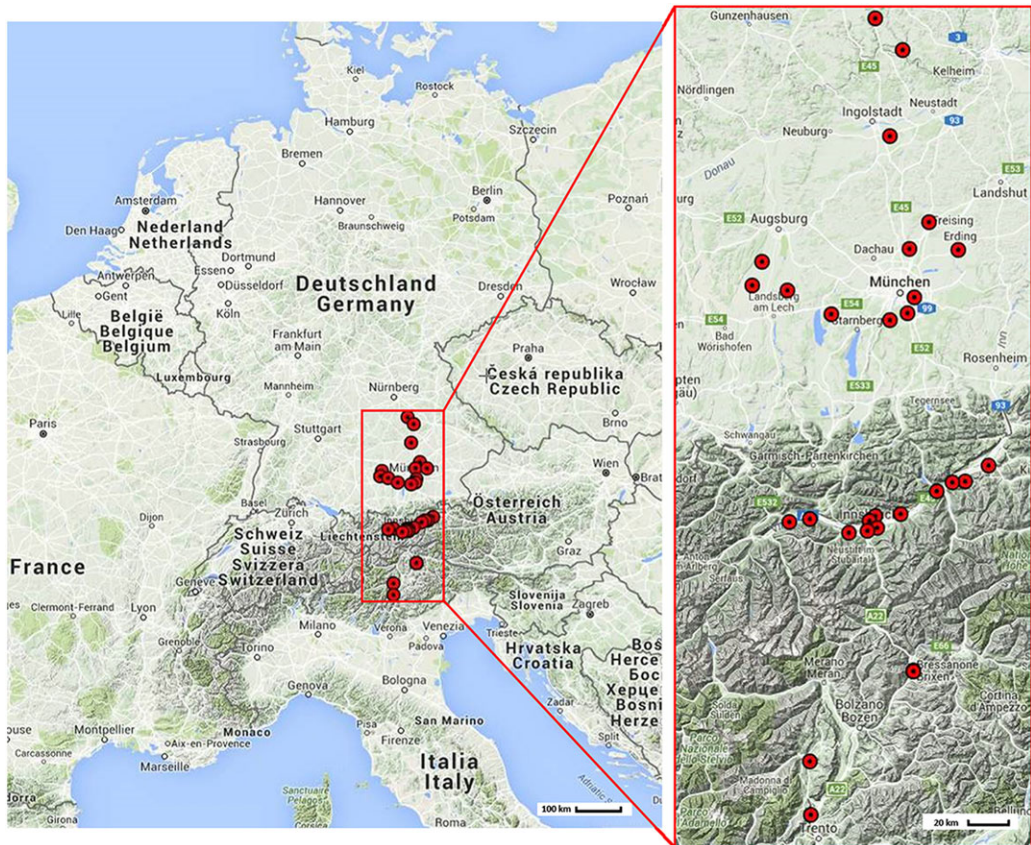


Figure 1 Sampling sites across the transalpine Inn–Eisack–Adige passage. For site codes and geographical coordinates from north to south, see Table 1. Source: A. Toncala with the use of a scribble map. [Colour figure can be viewed at wileyonlinelibrary.com]

of the rich ore deposits. In Antiquity, the Inn–Eisack–Adige passage was one of the most frequently used transalpine routes from south to north, and vice versa. The isotope measurements were performed in the frame of an isotopic mapping of this particular transect aiming at answering open archaeological questions related to transalpine mobility and culture transfer (www.for1670-transalpine.uni-muenchen.de). The differentiation between local and non-local finds was attempted by the application of a multi-isotope fingerprint consisting of $\delta^{18}\text{O}_{\text{phosphate}}$, $^{87}\text{Sr}/^{86}\text{Sr}$, $^{208}\text{Pb}/^{204}\text{Pb}$, $^{207}\text{Pb}/^{204}\text{Pb}$, $^{206}\text{Pb}/^{204}\text{Pb}$, $^{208}\text{Pb}/^{207}\text{Pb}$ and $^{206}\text{Pb}/^{207}\text{Pb}$ (Grupe *et al.* 2017). Since $\delta^{18}\text{O}_{\text{precipitation}}$ in the chosen reference area is affected by both latitude and, in particular, altitude, one focus of the study was the evaluation of the structural significance of $\delta^{18}\text{O}$ in the isotopic fingerprint.

The European Alps reach from south-east France to Austria and Slovenia, thereby covering a length of about 1000 km. The north-to-south dimension averages 200 km. Geologically, the mountains are divided into the western and eastern Alps. The latter extend from Switzerland and Germany to Austria covering geographical coordinates from 45 to 48°N and from 9 to 16°E, and have lower altitudes than the western Alps (Park 2014). While the northern and southern Alpine regions are dominated by soils developed on carbonate rocks, the inner Alpine area is mainly characterized by soils on crystalline parent material with higher $^{87}\text{Sr}/^{86}\text{Sr}$ isotopic ratios. Typical stable Pb isotopic ratios of alpine ore deposits and estimates of the spatial distribution of preindustrial isotopic ratios have been published by, for example, Durali-Mueller *et al.* (2007) and Artioli *et al.* (2016). Although the Brenner Pass (coordinates 47°0'N, 11°30'E) is one of the lowest passes across the alpine divide with an altitude of 1370 metres above sea level (m.a.s.l.) only, it was expected that especially $\delta^{18}\text{O}$ could serve as a suitable ecogeographical marker owing to the vertical differentiation of the region. Accompanying modern ecological reference samples taken from the archaeological sites from which the animal skeletons were sampled (in particular, ground and spring water, α -cellulose of hazelnut wood) in fact revealed an altitude effect (Göhring *et al.* 2015) of -0.18‰ per 100 m which is in very good agreement with the average altitude effect in the Alps measured in precipitation (-0.16‰ per 100 m; Humer *et al.* 1995). According to Kern *et al.* (2014), $\delta^{18}\text{O}$ in precipitation in the Alps correlates linearly with altitude until about 2000 m a.s.l.

In an initial phase of our project, we tested whether $\delta^{18}\text{O}_{\text{phosphate}}$ in a subsample ($n = 118$) of the animal bone specimens in fact exhibits the expected altitude effect. A highly significant correlation ($r = -0.68$) between average $\delta^{18}\text{O}_{\text{phosphate}}$ and altitude was found ($\delta^{18}\text{O}_{\text{precipitation}} = [-0.0030 \pm 0.0014] \times \text{altitude} - [7.95 \pm 0.77]$; Mayr *et al.* 2016), whereby mean $\delta^{18}\text{O}_{\text{phosphate}}$ values per site plotted on the regression between altitude and $\delta^{18}\text{O}$ in precipitation in the Alps ($\delta^{18}\text{O}_{\text{meteoric water}} = -0.0034 \times \text{altitude} - 7.79$; Kern *et al.* 2014). However, interindividual variability remained high and did not permit for a firm assignment of individual animals to a definite altitude (Mayr *et al.* 2016). This should be largely due to physiological, environmental and even cultural parameters (Lightfoot and O'Connell 2016).

Under the assumption that individuals that shared the same habitat during their lifetime exhibit similar local multi-isotopic fingerprints, we wanted to evaluate how meaningful $\delta^{18}\text{O}$ was compared with Sr and Pb isotopic ratios. In recent times, such fingerprints have been evaluated by use of mathematical tools such as hierarchical clustering (e.g., Turner *et al.* 2009; Keller *et al.* 2016). In this paper, data-mining techniques were employed to analyse multi-isotope data in order to evaluate which of the isotopic ratios (O, Sr, Pb) was the most relevant for isotope cluster analysis in the alpine reference region. While $\delta^{18}\text{O}$ reflects the altitude effect, geological north-to-south gradients were evidenced with regard to $^{87}\text{Sr}/^{86}\text{Sr}$, $^{207}\text{Pb}/^{204}\text{Pb}$ and $^{206}\text{Pb}/^{204}\text{Pb}$ as expected (Toncala *et al.* 2017).

MATERIALS AND METHODS

A total of 217 animal bones and two dentine samples from 30 archaeological sites (Tab. S1 and Fig. 1) were analysed for an isotopic map in terms of $\delta^{18}\text{O}_{\text{phosphate}}$, $^{87}\text{Sr}/^{86}\text{Sr}$, $^{208}\text{Pb}/^{204}\text{Pb}$, $^{207}\text{Pb}/^{204}\text{Pb}$, $^{206}\text{Pb}/^{204}\text{Pb}$, $^{208}\text{Pb}/^{207}\text{Pb}$ and $^{206}\text{Pb}/^{207}\text{Pb}$. The minimum number of individuals per site was three (site code 230). Three species were chosen, namely the domesticates cattle (*Bos taurus*, $n = 89$) and pig (*Sus domesticus*, $n = 82$), and red deer (*Cervus elaphus*, $n = 48$) as a representative of game. It was assumed that the domesticates were mainly kept in the vicinity of human dwellings, what could afterwards only be excluded for pigs from a single site (see the discussion). The bones were dated between 4500 BC and 300 AD (Tab. S1) according to the archaeological find contexts.

This manuscript focuses on the significance of $\delta^{18}\text{O}_{\text{phosphate}}$ as part of a multi-isotope fingerprint of archaeological animal bone apatite, assessed by data-mining methods. Therefore, the laboratory protocols for Sr and Pb isotope analysis and the respective measurement data are provided as supporting information online. For the complete isotopic map of the alpine transect, including detailed laboratory protocols, see Toncala *et al.* (2017).

 $\delta^{18}\text{O}$: sample processing and mass spectrometry

Sample preparation followed a modified procedure first published by L  quyer *et al.* (1993). The surfaces of the bone and tooth specimens were manually removed with tweezers and tongs to avoid any heat generation by grinding. Next, the samples were homogenized to a fine powder. For the deproteination, about 100 mg of bone powder were incubated in 5 ml of 4% NaOCl and kept under constant motion for at least two days. On the third day latest, the solution was changed and the incubation continued until effervescence ceased. The sample was then centrifuged at 5000 rpm for 5 min and washed with de-ionized water until pH 5–6. The pellet was re-suspended in 5 ml 1 M Ca acetate-acetic acid buffer (pH 4.5) and kept under constant motion for at least one day, followed by centrifuging and washing as described above, and lyophilized.

For the precipitation of silver phosphate, 3 mg apatite powder were weighted into 2 ml Eppendorf Safe-Lock tubes, 115 μl 2 M hydrofluoric acid (HF) were added and the samples kept under constant motion for at least 4 h. Next, 115 μl 2 M KOH were added to neutralize the solution, which was then centrifuged at 3000 rpm for 15 min. The supernatant was pipetted into a new tube and 1500 μl of AgNO_3 solution (pH 10–11) were added. The open tube was kept overnight at 60 $^\circ\text{C}$. On the following day, the supernatant (pH 6–7) was pipetted away and discarded, the silver phosphate crystals were washed carefully with distilled water, and the tubes were placed five times for 3 min each into an ultrasonic bath to loosen the remaining crystals from the tube walls. As much liquid as possible was pipetted away, and the crystals were dried in open tubes in an oven at 60 $^\circ\text{C}$ to a constant weight. Finally, the crystals were crunched. For the mass spectrometry, three times 0.93 mg each of the homogenized crystals per sample were weighted into tin capsules and vacuum dried at 60 $^\circ\text{C}$ for 48 h. Triplicate measurements were performed per sample accordingly.

The dried samples were immediately transferred to an autosampler flushed with helium and successively pyrolyzed in a HEKAtech HT Oxygen Analyser. Quantitative pyrolysis was achieved in a SiC reaction tube at 1490 $^\circ\text{C}$ in the presence of glassy carbon covered with a thin layer of granulated carbon. The resulting carbon monoxide was transferred in a continuous He flow via a trap filled with Carbosorb and MgClO_4 (both HEKAtech) and a gas chromatography column (GC, 70 $^\circ\text{C}$) to the mass spectrometer (Delta V Advantage, Thermo Fisher Scientific). The stable O isotope ratios are reported in the common delta notation as $\delta^{18}\text{O}$ (Vienna Standard Mean Ocean Water (VSMOW)). Analytical precision was 0.2‰ (1 SD).

$\delta^{18}\text{O}_{\text{phosphate}}$ was calculated from the m/z ratios 30 and 28 recorded in the mass spectrometer, and by use of the international benzoic acid standards IAEA 601 ($\delta^{18}\text{O} = 23.3\text{‰}$) and IAEA 602 ($\delta^{18}\text{O} = 71.4\text{‰}$). A phosphorite rock standard (NBS 120c) and bone ash (SRM 1400) that had both been processed in the same way as the samples had $\delta^{18}\text{O}$ values of 22.6‰ ($n = 21$) and 17.1‰ ($n = 23$) respectively. The $\delta^{18}\text{O}$ value of NBS 120c agreed with previously reported values of $22.6\text{‰} \pm 0.1\text{‰}$ (Vennemann *et al.* 2002) and $22.4\text{‰} \pm 0.2\text{‰}$ (Fischer *et al.* 2013), but disagreed with lower values reported in other publications (see Fischer *et al.* 2013 for discussion). Such differences may arise from different calibration standards, phosphate extraction protocols or methods and devices for isotope analyses (Vennemann *et al.* 2002). Triplicate analyses of 24 bone phosphate samples revealed an average standard deviation (SD) of 0.12‰ . All measurement data are listed in Table S1. Quality control for $^{87}\text{Sr}/^{86}\text{Sr}$ isotopic ratios was performed by use of the reference material SRM 987 ($^{87}\text{Sr}/^{86}\text{Sr}: 0.710219 \pm 0.000059$, $n = 80$), and for Pb isotopic ratios by use of NBS 982 ($^{206}\text{Pb}/^{204}\text{Pb} = 36.75842 \pm 0.03473$, $^{206}\text{Pb}/^{207}\text{Pb} = 2.14129 \pm 0.00087$, $n = 83$) (Toncala *et al.* 2017).

For the cluster analysis, $\delta^{18}\text{O}_{\text{phosphate}}$ values were converted into $\delta^{18}\text{O}_{\text{precipitation}}$ according to the regressions of Longinelli (1984) and D'Angela and Longinelli (1990). This way, species-specific physiological peculiarities were compensated for, and the measurement data of all three species were lumped together (Mayr *et al.* 2016).

Data-mining

Knowledge discovery in databases (KDD) is the process of extracting knowledge from raw data through data-mining techniques. Feature selection is a critical part of the KDD process and the data-mining results depend heavily on the selected feature space. In this case, features per individual animal bone include all isotopic ratios, and the geographical site's coordinates. Not all collected features need to be important for an analysis task because they might be irrelevant for the specific analysis, noisy or redundant due to the existence of other features in the data description. In our case, we wanted to evaluate the importance of the different isotope ratios and, in particular, of $\delta^{18}\text{O}$.

There is a variety of methods and techniques for feature selection in the data-mining area (Guyon and Elisseeff 2013). However, most of the approaches refer to the supervised learning case and require class information for feature evaluation. In our case, there is no class information and, therefore, we investigated feature selection as an unsupervised learning task. Our approach belongs to the general category of wrapper methods for feature selection. The feature quality is evaluated through a learning algorithm and, in particular, through clustering.

We examined how relevant a feature is for a clustering result and proposed a stability-based ranking of the features. The concept of stability is used to measure (clustering) structure preservation after omitting a feature. To evaluate stability, we employed the notions of structural relevance and structural redundancy of a feature for a reference clustering. The *structural relevance* of a feature reflects the agreement of the clustering obtained using only this feature compared with the reference clustering. Except for the structural relevance that focuses on a single attribute's contribution to a reference clustering, we also incorporated the *structural redundancy* of the feature by examining how well the complementary feature space, i.e., the rest of the features in the data description, captured the reference clustering structure. As a *reference clustering* for the comparison, in the absence of any ground truth, we used the full dimensional clustering extracted upon all different isotope ratios. For the clustering part, we used the expectation–

maximization (EM) algorithm (Dempster *et al.* 1977); the exact clustering process and extracted clusters are discussed in detail by Mauder *et al.* (2016a, 2016b).

More formally, let $F = \langle \delta^{18}\text{O}, {}^{87}\text{Sr}/{}^{86}\text{Sr}, {}^{208}\text{Pb}/{}^{204}\text{Pb}, {}^{207}\text{Pb}/{}^{204}\text{Pb}, {}^{206}\text{Pb}/{}^{204}\text{Pb}, {}^{208}\text{Pb}/{}^{207}\text{Pb}, {}^{206}\text{Pb}/{}^{207}\text{Pb} \rangle$ be the isotopic feature space and let D be the data set described in the aforementioned feature space. Let Θ^F be the reference clustering, extracted by applying the EM clustering algorithm upon D . The result of clustering is a set of disjoint clusters, $\Theta^F = \{\theta_1, \theta_2, \dots, \theta_k\}$, where k is the number of clusters. Let $f \in F$ be a single feature whose effect on clustering Θ^F we want to evaluate. Let D^f be the original data set projected only onto dimension f ; and let Θ^f be the clustering over D^f : $\Theta^f = \{\theta_1, \theta_2, \dots, \theta_{k'}\}$, where k' is the number of clusters. We refer to Θ^f as *univariate clustering*. Let $f^c = F \setminus \{f\}$ be the complementary feature space, that is, all dimensions in F except for the investigated feature f . Let D^{f^c} be the complementary data set, i.e., the data set projected onto the complementary feature space f^c . Applying EM in D^{f^c} results in a clustering $\Theta^{f^c} = \{\theta_1, \theta_2, \dots, \theta_{k''}\}$ where k'' is the number of clusters. We refer to Θ^{f^c} as *complementary clustering*.

To evaluate the effect of a single feature f on the reference clustering structure Θ^F , we compare the univariate clustering Θ^f derived from the specific feature f and the complementary clustering Θ^{f^c} derived from the complementary feature space f^c with the reference clustering Θ^F . The first comparison evaluates the contribution of f to Θ^F , whereas the second evaluates whether f 's contribution can be replicated by some other feature(s) in the feature space. In that sense, the first score derives the specific feature's *structural relevance* and the second score its *structural redundancy* owing to the existence of other feature(s) in the feature space.

For comparison, we employ the adjusted Rand index (ARI) that evaluates the agreement between two clusterings by counting pairs assigned to the same cluster under both clusterings and pairs assigned to different clusters versus the total number of pairs in the data set. We derive two rankings from the ARI scores for the single features and their complementary feature spaces, referred to as the *univariate ranking* R and *complementary ranking* R^c . Combining univariate clustering (structural relevance) and complementary clustering (structural redundancy) scores in a single score is not straightforward owing to the different semantics of the rankings. For this reason, we propose to generate these rankings separately and characterize each feature f in terms of both structural relevance and redundancy. In particular, we propose a *relevance versus redundancy feature characterization plot*: the x -axis shows the agreement of univariate clustering to the reference clustering, whereas the y -axis refers to the complementary clustering agreement scores with regard to the reference clustering. In other words, the x -axis represents the degree to which the reference clustering structure is evident in a single dimension and, therefore, is a measure of f 's relativity, while the y -axis shows whether the reference clustering structure can be captured by the rest of the dimensions and, therefore, is a measure of f 's redundancy.

RESULTS

Total variability of stable isotopic ratios among all 219 individual mammals is 12.5–17.1‰ for $\delta^{18}\text{O}$, 0.70708–0.72068 for ${}^{87}\text{Sr}/{}^{86}\text{Sr}$, 38.1878–38.8265 for ${}^{208}\text{Pb}/{}^{204}\text{Pb}$, 15.6043–15.8570 for ${}^{207}\text{Pb}/{}^{204}\text{Pb}$, 18.3299–21.3966 for ${}^{206}\text{Pb}/{}^{204}\text{Pb}$, 2.4081–2.4766 for ${}^{208}\text{Pb}/{}^{207}\text{Pb}$, and 1.1722–1.3492 for ${}^{206}\text{Pb}/{}^{207}\text{Pb}$. A subsample of 63 bones was investigated by both X-ray diffraction (XRD) and Fourier-transform infrared spectrometry (FTIR), two complementary methods commonly applied for mineralogical homogeneity tests. Especially, modern XRD has been successfully performed for the evaluation of crystallographic characteristics of archaeological and fossil bones (Stathopoulou *et al.* 2008; Piga *et al.* 2009). Only a single mineral phase (hydroxyapatite)

was detectable, and no contaminants. Minor diagenetic alterations concerned a probable exchange of carbonate by hydroxyl or fluorine and did not relate to the isotopes measured in this study. Microstrain, a result of inhomogeneities in the mineral composition and lattice defects on the scale of the crystallite size, was explicitly monitored with regard to the ongoing debate on the reliability of both XRD and FTIR (Schmahl *et al.* 2016, 2017). Stable Pb isotopic ratios in the bones match the respective values measured in prehistoric peat bog layers (e.g., Shotyk *et al.* 1998; Breitenlechner *et al.* 2010; Kamenov and Gulson 2014) and do not exhibit any contamination, e.g., due to modern pollution. Therefore, we assumed that the sample processing protocol successfully decontaminated the samples and that the measured isotopic ratios reflected the original biogenic signals. This assumption is strongly supported by the variability of $^{87}\text{Sr}/^{86}\text{Sr}$ isotopic ratios measured in animals recovered from the same site (Fig. S1 and Tab. S2). Site-specific variability of $^{87}\text{Sr}/^{86}\text{Sr}$ ratios in the animal bones of this study varied between 0.00037 (site 116), matching the variability in a local population (Burton and Price 2013), and 0.00889 (site 312), a spacing that highly exceeds even most conservative differentiations between local and non-local signals (average ± 2 SD, or average ± 0.001 ; Grupe *et al.* 1997). Distances covered by the home ranges of game and different herding practices for domesticates in regions with a small-scale variability of local Sr isotopic ratios such as the Alps and alpine foothills are responsible for these spacings, which can, however, no more result from contamination by the burial environment. Moreover, according to Söllner *et al.* (2016) and Crowley *et al.* (2017), $^{87}\text{Sr}/^{86}\text{Sr}$ in the bones of large vertebrates is more strongly related to local water sources than to the soil.

Stable O isotopic ratios exhibit a considerable variability, but a clear depression at higher altitudes (Fig. 2 and Tab. S1) (see also Mayr *et al.* 2016). Because of this, and the perfect match of the regressions of Mayr *et al.* (2016) and Kern *et al.* (2014), we conclude that the general altitude effect of $\delta^{18}\text{O}$ in precipitation of the alpine transect is adequately integrated by the $\delta^{18}\text{O}_{\text{phosphate}}$ of the archaeological vertebrates. Variability per site can, however, be conspicuous (0.1–3.0‰ in cattle, 0.1–2.0‰ in pigs, and 0–4.0‰ in red deer; Tab. 1).

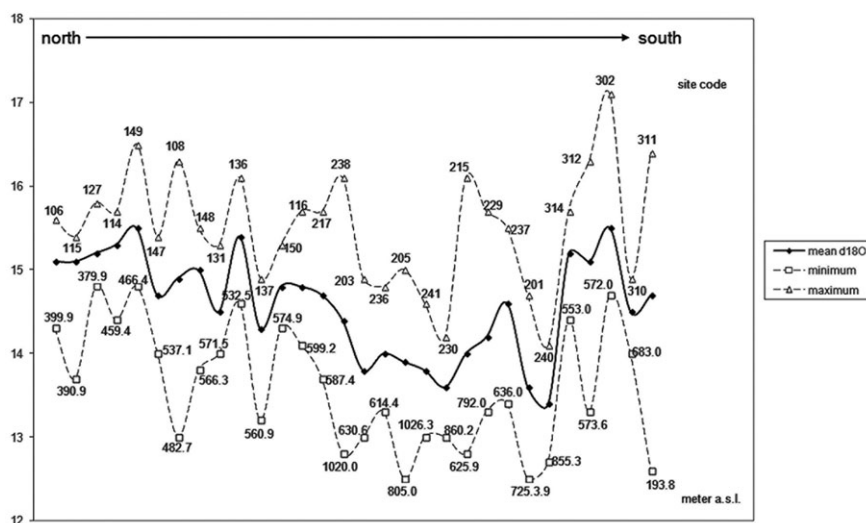


Figure 2 Average, minimum and maximum $\delta^{18}\text{O}_{\text{phosphate}}$ in animal bones per site in a north-to-south direction across the transalpine passage. Site codes are indicated next to the maximums; altitude (meters above sea level—m a.s.l.) is indicated next to the minimums.

Table 1 Interindividual variability of $\delta^{18}\text{O}_{\text{phosphate}}$ per species and site ($\Delta\delta^{18}\text{O}$) (‰)

Site code	$\Delta\delta^{18}\text{O}$ cattle	$\Delta\delta^{18}\text{O}$ pig	$\Delta\delta^{18}\text{O}$ red deer
106	0.8	0.8	0.8
115	1.7	0.4	0.5
127	1	0.1	0.8
114	1.3	0.5	0.9
149	0.7	0.3	0.6
147	1	1.4	1.2
108	1.4	2	1.3
148	0.4	1.6	
131	0.8	0.4	1
136	0.1	1.5	
137	0.2	0.3	0.9
150	0.8	0.7	
116	0.9	0.4	
217	1.6	1.5	
238	1.2	1.2	
203	1.3		0
236	0.8	0.9	
205/206	0.8	1.4	
241	0.3	1.2	0.4
230	1.2		
215	3	1.2	
229	0.6	1.8	0.2
237	0.5	1.9	
201	1.8	1.2	
240	1.4	0.8	0.9
314	0.2		
312	3	1.5	
301	1	1	2.2
310	0.8	0.6	
311	1.3	0.5	4

The question maintains whether $\delta^{18}\text{O}_{\text{phosphate}}$ is an indispensable feature of the multi-isotope fingerprint for the establishment of the regional isotopic map. The common bivariate plot of $\delta^{18}\text{O}_{\text{phosphate}}$ against $^{87}\text{Sr}/^{86}\text{Sr}$ in bone apatite exhibits some clustering of both Sr and O isotopic ratios in the areas to the north and south of the Alps, and the inner-alpine sites (Fig. 3). However, site-specific variability is still too high to permit a firm spatial allocation of individual animals with the exception of a few singular cases.

Statistical analyses mostly need an a priori definition of data groups that can be compared with each other in terms of descriptive features. A common procedure is analysis of variance (ANOVA) that tests whether significant differences exist between at least two expectation values. By using the spatial location of the sites to the north and south of the Alps, and the inner-alpine region as group labels, significant differences were found for all isotopic ratios ($\delta^{18}\text{O}$: $F = 41.53$, $p \leq 0.001$; $^{87}\text{Sr}/^{86}\text{Sr}$: $F = 59.75$, $p < 0.001$; $^{208}\text{Pb}/^{204}\text{Pb}$: $F = 7.49$, $p < 0.001$; $^{207}\text{Pb}/^{204}\text{Pb}$: $F = 3.68$, $p = 0.027$; $^{206}\text{Pb}/^{204}\text{Pb}$: $F = 19.40$, $p < 0.001$), whereby the inner-alpine region is characterized by lower $\delta^{18}\text{O}$ values (Fig. 2). A north-to-south or south-to-north gradient was depictable for Sr and Pb isotopic ratios (see also Toncala *et al.* 2017).

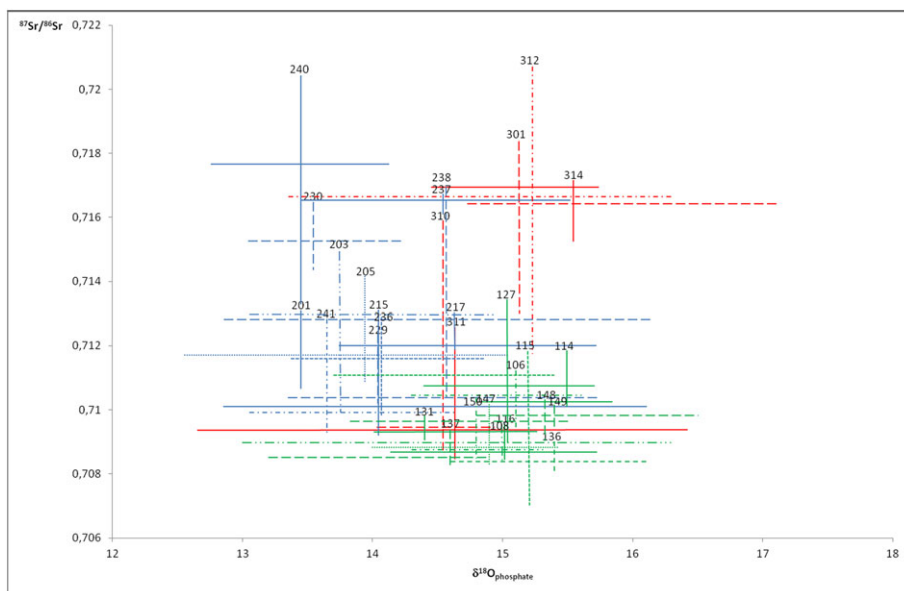


Figure 3 Bivariate plot of $\delta^{18}\text{O}_{\text{phosphate}}$ against $^{87}\text{Sr}/^{86}\text{Sr}$ (medians, minimums and maximums) in all animal bones. Sites to the north of the Alps have site codes that start with 1; inner-alpine site labels start with 2; and southern alpine site codes start with 3 (see Tab. S1). [Colour figure can be viewed at wileyonlinelibrary.com]

Principal component analysis (PCA) is another valuable tool used to reduce the dimensions of a data set and evaluate the explanatory power of its components. In our data set, five components were capable of explaining a variance $> 1\%$ each (components 0–4: 0.5111, 0.1865, 0.1502, 0.1214 and 0.0308 respectively). The PCA is dominated by the Pb isotopic ratios and shows that $\delta^{18}\text{O}$ plays a role for the third and fourth components only (Tab. 2 and Fig. S2). Therefore, it is hard to define the importance of a single feature within the multi-isotope fingerprint by common multivariate approaches. We applied a Gaussian mixture model (GMM) clustering to solve this question by either adding or omitting spatial information.

The structure of the following data sets was analysed by use of GMM and the EM algorithm: the complete data set includes $\delta^{18}\text{O}_{\text{phosphate}}$, $^{87}\text{Sr}/^{86}\text{Sr}$, $^{208}\text{Pb}/^{204}\text{Pb}$, $^{207}\text{Pb}/^{204}\text{Pb}$, $^{206}\text{Pb}/^{204}\text{Pb}$, and the commonly reported Pb isotopic ratios $^{208}\text{Pb}/^{207}\text{Pb}$ and $^{206}\text{Pb}/^{207}\text{Pb}$ (seven features). To test for the relative importance versus redundancy, analyses were repeated after omitting $\delta^{18}\text{O}$ (six features). To reveal the spatial information hidden in each isotopic ratio measured in the bone apatite, two additional features spaces were generated (one with and one without $\delta^{18}\text{O}$), where the

Table 2 Results of the principal component analysis (PCA)

Component	$\delta^{18}\text{O}$	$^{87}\text{Sr}/^{86}\text{Sr}$	$^{208}\text{Pb}/^{204}\text{Pb}$	$^{207}\text{Pb}/^{204}\text{Pb}$	$^{206}\text{Pb}/^{204}\text{Pb}$	$^{208}\text{Pb}/^{207}\text{Pb}$	$^{206}\text{Pb}/^{207}\text{Pb}$
0	0.052444	-0.171279	-0.212997	0.445913	0.505582	-0.464295	-0.505582
1	-0.258730	-0.056416	-0.779723	-0.347151	-0.188268	-0.371068	-0.168102
2	-0.751023	0.612444	0.112724	0.197889	0.065882	-0.047249	0.049368
3	0.603014	0.762434	-0.184638	0.005052	-0.010849	-0.144116	-0.008061
4	0.051413	-0.105294	0.084999	0.646926	-0.401155	-0.366960	-0.514730

spatial information of the site coordinates where the bones had been excavated (latitude, longitude, altitude) was included. These feature spaces constitute the best starting point because they include the most information available. Figs 4 and 5 plot the structural relevance against the respective structural redundancy each.

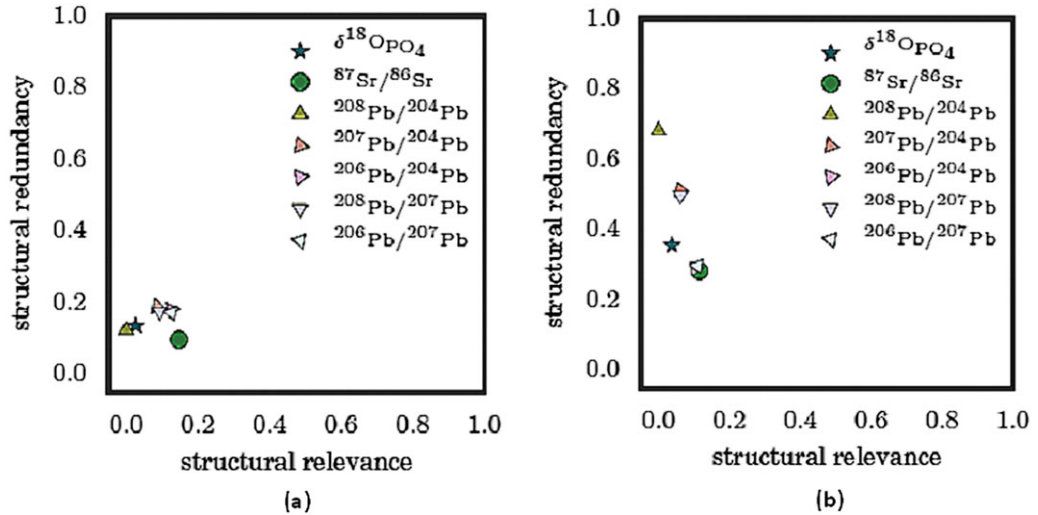


Figure 4 (a) Structural relevance versus structural redundancy of all isotopic ratios including spatial information (longitude, latitude, altitude); and (b) structural relevance versus structural redundancy of isotopic ratios without any spatial information. [Colour figure can be viewed at wileyonlinelibrary.com]

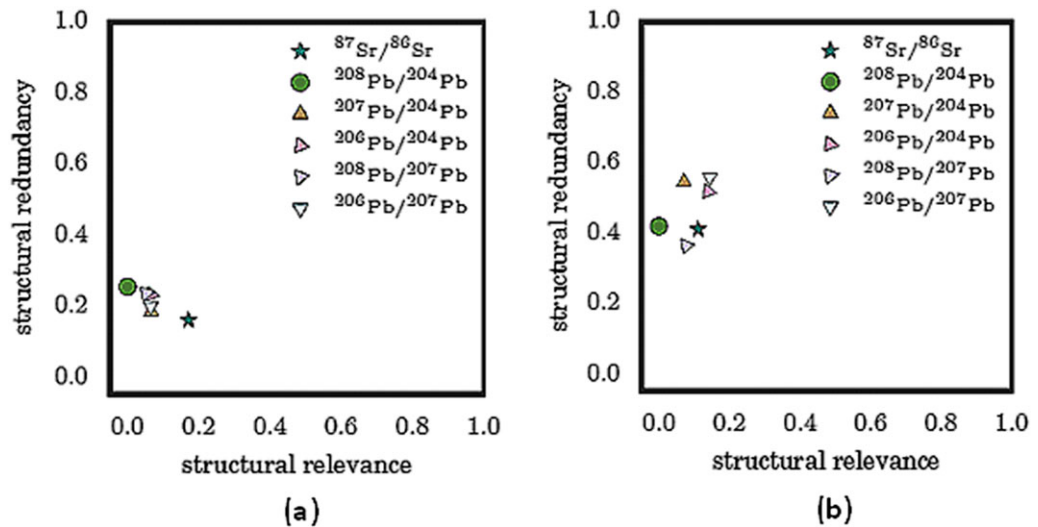


Figure 5 (a) Structural relevance versus structural redundancy of isotopic ratios excluding $\delta^{18}\text{O}$, but including spatial information (longitude, latitude, altitude); and (b) structural relevance versus structural redundancy of isotopic ratios excluding $\delta^{18}\text{O}$, and also excluding spatial information (longitude, latitude, altitude). [Colour figure can be viewed at wileyonlinelibrary.com]

When the spatial information is added (Fig. 4 (a)), $^{87}\text{Sr}/^{86}\text{Sr}$ is the most important attribute because it exhibits the highest structural relevance score. Lowest relevance scores are shared by $^{208}\text{Pb}/^{204}\text{Pb}$ and $\delta^{18}\text{O}$, while the other Pb isotopic ratios are of equal relevance but of slightly higher redundancy. Considering the isotopic ratios only without any spatial information (Fig. 4 (b)), the structural redundancy of all isotopic ratios rises considerably, whereby $\delta^{18}\text{O}$ and some Pb isotopic ratios are most affected. $^{87}\text{Sr}/^{86}\text{Sr}$ remains the top relevant isotopic ratio within the feature space. $^{206}\text{Pb}/^{207}\text{Pb}$ and $^{206}\text{Pb}/^{204}\text{Pb}$ plot very close to each other and gain in relevance. The highest redundancy score is evidenced in $^{208}\text{Pb}/^{204}\text{Pb}$.

If $\delta^{18}\text{O}$ is omitted from the data set but the spatial information added (Fig. 5 (a)), $^{87}\text{Sr}/^{86}\text{Sr}$ remains the most important feature, but the structural relevance of all Pb isotopic ratios decreases. Again, $^{208}\text{Pb}/^{204}\text{Pb}$ is the least informative and most redundant attribute. After removal of the spatial information (Fig. 5 (b)), Pb isotopic ratios except $^{208}\text{Pb}/^{204}\text{Pb}$ gain in relevance, but are mostly more redundant than $^{87}\text{Sr}/^{86}\text{Sr}$.

It is clear that Sr and Pb isotopic ratios are the top relevant features of our data set, while $\delta^{18}\text{O}$ is of considerably lower relevance. It should be emphasized that all isotopic ratios do not have very high relevance scores in each of the four experiments, which implies that no isotopic ratio alone is capable of reflecting the full structure of the data set. This is in perfect agreement with the known spatial redundancy of single isotopes, and supports the necessity of multi-isotope fingerprints for provenance studies. The relevance of $\delta^{18}\text{O}$ does not obviously dominate the structure of the data set, although its redundancy is not particularly low when compared with the other features. $\delta^{18}\text{O}$ does exhibit the altitude effect (see above), but with regard to the overall spatial make-up of the reference area studied, omitting $\delta^{18}\text{O}$ from the feature space does not diminish the results substantially. It needs to be emphasized, however, that the information hidden in $\delta^{18}\text{O}$ is thereby lost. Since this study focuses on the similarity of individual multi-isotope fingerprints for archaeological provenance studies in a specific area, this loss should be tolerable. If specific questions such as, for example, herding practices in alpine environments (transhumance), are addressed, individual $\delta^{18}\text{O}$ values might well be of even higher importance than other isotopic ratios.

DISCUSSION

Since the reference area chosen for the isotopic map is located in the European Alps, both latitude and especially altitude effects manifested in the $\delta^{18}\text{O}$ values were expected. As stated above, these effects were indeed detectable in modern environmental samples (Göhring *et al.* 2015), and in the means of the subsample of animal bones of Mayr *et al.* (2016). Deciphering the general spatial information hidden in apatite stable isotopic ratios of bioarchaeological finds from the chosen region is, however, not jeopardized when $\delta^{18}\text{O}_{\text{phosphate}}$ is excluded from the multi-isotope fingerprint. With regard to the intra-individual variability of $\delta^{18}\text{O}_{\text{phosphate}}$, and the fact that regressions between $\delta^{18}\text{O}_{\text{precipitation}}$ and altitude can also be site specific (e.g., when a site is located in the wind shadow of high mountain chains; Humer *et al.* 1995), this result is no great surprise. While the results hold for the specific alpine transect of the Inn–Eisack–Adige passage, it is noteworthy that previous studies also failed to detect a clear correlation between individual $\delta^{18}\text{O}$ in bone apatite and place of origin in a mountainous region (e.g., Bentley and Knipper 2005). In our case, the limited suitability of $\delta^{18}\text{O}$ for the definition of place of provenance cannot simply be due to the limited precision of the existing hydrological maps for Europe (Bowen and Revenaugh 2003), since recent data for the European Alps have been made available by Kern

et al. (2014). Climatic shifts through time also need to be taken into account, but they should not obscure general latitude and altitude effects. This is why animal bone finds from different archaeological times had been chosen deliberately (Tab. S1). Therefore, other possible factors probably need consideration.

Pollard *et al.* (2011) recalculated published regressions between $\delta^{18}\text{O}_{\text{phosphate}}$ and $\delta^{18}\text{O}_{\text{water}}$ for vertebrates including humans and ended up with 95% confidence intervals around 4%. This way, the uncertainty in calculated $\delta^{18}\text{O}_{\text{water}}$ values exceeds the total range of the known variability across the whole of western continental Europe and led the authors to suggest instead a direct $\delta^{18}\text{O}_{\text{phosphate}}$ mapping in order to detect non-local finds by the exclusion principle. Our cluster analysis revealed that $\delta^{18}\text{O}_{\text{phosphate}}$ did not contribute substantial information beyond stable Sr and Pb ratios in the case of the transalpine passage. In contrast to the latter, $\delta^{18}\text{O}$ is independent of the geological underground, but rather strongly depends on geomorphology and atmospheric circulation. Therefore, the limitations of stable O isotopes with regard to cluster analysis in the reference area chosen in this study may well be a regional-specific phenomenon.

Another issue that needs to be addressed when working with bioarchaeological finds is diagenesis. While $\delta^{18}\text{O}$ in phosphate is in general more reliable than $\delta^{18}\text{O}$ in the bone structural carbonate (Lee-Thorp 2002), what could also be confirmed for our data by analysis of both $\delta^{18}\text{O}_{\text{phosphate}}$ and $\delta^{18}\text{O}_{\text{carbonate}}$ from a subsample ($n = 91$; Toncala *et al.* 2017), bone is a more delicate material than dental enamel in terms of its susceptibility to diagenetic alteration. While the widespread assumption that enamel should be resistant towards diagenetic alteration is definitely not true, which has been shown previously by Rink and Schwarcz (1995), it is nevertheless crucial to characterize systematically the analysed samples in terms of their mineralogical features, which was a central part of our study. Since compact bone integrates isotopic signatures incorporated into the skeleton over years, this tissue was deliberately chosen in the attempt of a spatial allocation of isotopic fingerprints.

In our opinion, the low structural relevance of $\delta^{18}\text{O}$ in our study is based on biological, environmental and also cultural parameters. Different vertebrate species integrate local $\delta^{18}\text{O}$ in drinking water in different ways. While red deer cover the major portion of drinking water from solid food, cattle and pigs need to drink regularly. Plant food sources vary considerably in $\delta^{18}\text{O}$, whereby leaves are in general enriched with ^{18}O , which can lead to significant differences in consumer $\delta^{18}\text{O}$ values in different species from the same site (Fricke *et al.* 1998). Deliberate feeding of domesticates and special types of herd management may be of influence on both the food and drinking water sources for cattle (alpine pastures) and pigs (human leftovers). Since baseline stable O isotope ratios are temperature related, different water sources should also be taken into account. A good example is the Zambana case (site code 311; Fig. 2), which is located at the lowest altitude of all the sites sampled for this study, and where the $\delta^{18}\text{O}_{\text{phosphate}}$ values of the pig bones exhibit particularly low values. Zambana is located in the Adige river valley in northern Italy, where the river water originates from high-altitude glaciers. Possibly the pigs had been raised in the vicinity of the river or indeed at higher altitudes and were not primarily local to the site of their recovery (Mayr *et al.* 2016). We can also not exclude fully that some individual animals had been imported to the sites of their discovery since the alpine transect via the Brenner Pass has been a busy communication network since prehistory (Lang 2002). Also, either the home ranges of free-ranging vertebrates such as the red deer, or the respective hunting grounds, were larger and more diverse than today. All these factors are likely to introduce some 'noise' into the overall isotopic variability.

Another parameter that is of no importance to the radiogenic isotopic ratios but which can be influential on $\delta^{18}\text{O}$ is the fact that the individual animals for certain did not die in the same year. The dating of the finds (Tab. S1) covers large time frames where changing weather conditions or

even climate fluctuations may have occurred. The imprint on $\delta^{18}\text{O}$ varies according to the environment and can be very pronounced in alpine regions (Humer *et al.* 1995; Schürch *et al.* 2003). While compact bone integrates the water consumption over the life time of the mammal and, therefore, also the variability of $\delta^{18}\text{O}$ between all seasons of a year, such integrated $\delta^{18}\text{O}$ may vary considerably in animals that had lived under different climatic conditions. All these parameters probably combine to give the observed high interindividual variability of $\delta^{18}\text{O}_{\text{phosphate}}$ per species and site (Tab. 2).

CONCLUSIONS

We investigated a transalpine reference area in terms of stable O, Sr and Pb isotopes in the bioapatite of archaeological animal bones in order to establish baseline values for the reconstruction of prehistoric mobility and trade. Following expectations with regard to the vertical stratification of the region, an altitude effect in $\delta^{18}\text{O}_{\text{phosphate}}$ was detectable, which was in total agreement with modern data on $\delta^{18}\text{O}$ in precipitation. To evaluate which of the isotopic ratios measured in the animal bone finds contained the most important spatial information, the isotopic fingerprints per individual were analysed by GMM clustering and an EM algorithm. It was shown that among the complete data set, the Sr and Pb isotopic ratios were the top relevant features and $\delta^{18}\text{O}$ was of considerably lower relevance. This is in accordance with Price *et al.* (2017), who claim that both the Sr and Pb isotopes in animal bone finds are suitable for provenance analyses because the animals will ‘fingerprint’ the local bioavailable Sr and the ‘nearest lead source’.

This opens new possibilities for bioarchaeological provenance studies in the chosen area. For long periods of human prehistory, cremating the dead was the common if not the exclusive burial practice. It has been shown experimentally that $\delta^{18}\text{O}_{\text{phosphate}}$ is significantly altered at high temperatures (Munro *et al.* 2008) and so is of no use for provenance studies. While $^{87}\text{Sr}/^{86}\text{Sr}$ in bone is thermally stable up to 1000 °C (Harbeck *et al.* 2011), this has not yet been shown experimentally for Pb isotopes to the best of our knowledge. Since the Pb atom is by far heavier than that of Sr, no heat-induced changes of Pb isotopic ratios should occur either. We do not intend to generalize our results and emphasize that they only hold for the specific region investigated so far, but provenance analysis based on cremated finds by the combination of Sr and Pb stable isotopes is generally possible. We also conclude that the application of data-mining methods opens new perspectives for the interpretation of the various isotopic systems applied for provenance analysis in terms of their predictive potential which is not recovered by common uni- and multivariate approaches.

ACKNOWLEDGMENTS

This study was supported financially by the Deutsche Forschungsgemeinschaft (Research Group FOR 1670). Special thanks to Dr Simon Trixl, Institute for Palaeoanatomy, Domestication Research and History of Veterinary Medicine, LMU Munich, for making the animal samples available.

REFERENCES

- Artioli, G., Angelini, I., Nimis, P., and Villa, I. M., 2016, A lead-isotope database of copper ores from the Southeastern Alps: a tool for the investigation of prehistoric copper metallurgy, *Journal of Archaeological Science*, **75**, 27–39.
- Ben-David, M., and Flaherty, E. A., 2012, Stable isotopes in mammalian research: a beginner’s guide, *Journal of Mammalogy*, **93**, 312–28.

- Bentley, R. A., and Knipper, C., 2005, Geographical patterns in biologically available strontium, carbon and oxygen isotope signatures in prehistoric SW Germany, *Archaeometry*, **47**, 629–44.
- Bowen, G. J., and Revenaugh, J., 2003, Interpolating the isotopic composition of modern meteoric precipitation, *Water Resources Research*, **39**(10), 1299, <https://doi.org/10.1029/2003WR002086>
- Breitenlechner, E., Hilber, M., Lutz, J., Kathrein, Y., Unterkircher, A., and Oeggle, K., 2010, The impact of mining activities on the environment reflected by pollen, charcoal and geochemical analyses, *Journal of Archaeological Science*, **37**, 1458–67.
- Bryant, J. D., and Froelich, P. N., 1995, A model of oxygen isotope fractionation in body water of large mammals, *Geochimica et Cosmochimica Acta*, **59**, 4523–37.
- Burton, J. H., and Price, T. D., 2013, Seeking the local $^{87}\text{Sr}/^{86}\text{Sr}$ ratio to determine geographic origins of humans: no easy answers, in *Archaeological chemistry VIII* (eds. R. A. Armitage and J. H. Burton), 309–20, American Chemical Society, Washington, DC.
- Crowley, B. E., Miller, J. H., and Bataille, C. P., 2017, Strontium isotopes ($^{87}\text{Sr}/^{86}\text{Sr}$) in terrestrial ecological and palaeoecological research: empirical efforts and recent advances in continental-scale models, *Biological Reviews*, **92**, 43–59.
- D'Angela, D., and Longinelli, A., 1990, Oxygen isotopes in living mammal's bone phosphate: further results, *Chemical Geology: Isotope Geoscience Section*, **86**, 75–82.
- Dansgaard, W., 1964, Stable isotopes in precipitation, *Tellus*, **16**, 436–68.
- Dempster, A. P., Laird, N. M., and Rubin, D. B., 1977, Maximum likelihood from incomplete data via the EM algorithm, *Journal of the Royal Statistical Society Series B (Methodological)*, **39**, 1–38.
- Durali-Mueller, S., Brey, G. P., Wigg-Wolf, D., and Lahaye, Y., 2007, Roman lead mining in Germany: its origin and development through time deduced from lead isotope provenance studies, *Journal of Archaeological Science*, **34**, 1555–67.
- Fischer, J., Schneider, J. W., Voigt, S., Joachimski, M. M., Tichomirowa, M., Tütken, T., Götze, J., and Berner, U., 2013, Oxygen and strontium isotopes from fossil shark teeth: environmental and ecological implication for Late Palaeozoic European basins, *Chemical Geology*, **342**, 44–62.
- Fricke, H. C., Clyde, W. C., and O'Neil, J. R., 1998, Intra-tooth variations in $\delta^{18}\text{O}$ (PO_4) of mammalian tooth enamel as a record of seasonal variations in continental climate variables, *Geochimica et Cosmochimica Acta*, **62**, 1839–50.
- Gat, J. R., 1996, Oxygen and hydrogen isotopes in the hydrologic cycle, *Annual Reviews of Earth and Planetary Science*, **24**, 225–62.
- Göhring, A. B., Toncala, A., Mayr, C., Söllner, F., and Grupe, G., 2015, Stable oxygen isotope mapping of the transalpine Inn–Eisack–Etsch passage based on modern α -cellulose and water, *Documenta Archaeobiologiae*, **12**, 53–80.
- Grupe, G., Grigat, A., and McGlynn, G. C., 2017, *Across the Alps in prehistory—Isotopic mapping of the Brenner Passage by bioarchaeology*, Springer, Cham.
- Grupe, G., Price, T. D., Schröter, P., Söllner, F., Johnson, C. M., and Beard, B. L., 1997, Mobility of Bell Beaker people revealed by strontium isotope ratios of tooth and bone: a study of southern Bavarian skeletal remains, *Applied Geochemistry*, **12**, 517–25.
- Guyon, I., and Elisseeff, A., 2013, An introduction to variable and feature selection, *Journal of Machine Learning Research*, **3**, 1157–82.
- Harbeck, M., Schleuder, R., Schneider, J., Wiechmann, I., Schmahl, W. W., and Grupe, G., 2011, Research potential and limitations of trace analyses of cremated remains, *Forensic Science International*, **204**, 191–200.
- Horita, J., and Wesolowski, D. J., 1994, Liquid–vapor fractionation of oxygen and hydrogen isotopes of water from the freezing to the critical temperature, *Geochimica et Cosmochimica Acta*, **58**, 3425–37.
- Humer, G., Rank, D., and Stihler, W., 1995, *Niederschlagsisotopennetzwerk Österreich*, Monographien des Bundesministeriums für Umwelt, Band 52, Vienna.
- Kamenov, G. D., and Gulson, B. L., 2014, The Pb isotopic record of historical to modern human lead exposure, *Science of the Total Environment*, **490**, 861–70.
- Keller, A. T., Regan, L. A., Lundstrom, C. C., and Bower, N. W., 2016, Evaluation of the efficacy of spatiotemporal Pb isoscapes for provenancing of human remains, *Forensic Science International*, **261**, 83–92.
- Kern, Z., Kohán, B., and Leuenberger, M., 2014, Precipitation isoscape of high reliefs: interpolation scheme designed and tested for monthly resolved precipitation oxygen isotope records of an Alpine domain, *Atmospheric Chemistry and Physics*, **14**, 1897–907.
- Kohn, M. J., 1996, Predicting animal $\delta^{18}\text{O}$. Accounting for diet and physiological adaptation, *Geochimica et Cosmochimica Acta*, (23), 4811–29.
- Kohn, M. J., and Cerling, T. E., 2002, Stable isotope compositions of biological apatite, *Reviews in Mineralogy and Geochemistry*, **48**, 455–88.

- Lang, A., 2002, Das Inntal als Route für Verkehr und Handel in der Eisenzeit, in *Über die Alpen* (ed. G. Schnekenburger), 49–55, Menschen-Wege-Waren, Archäologisches Landesmuseum Baden-Württemberg, Stuttgart.
- Lee-Thorp, J., 2002, Two decades of progress towards understanding fossilization processes and isotopic signals in calcified tissue material, *Archaeometry*, **44**, 435–46.
- Léquer, C., Grandjean, P., O'Neil, J. R., Capetta, H., and Marineau, F., 1993, Thermal excursions in the ocean at the Cretaceous–Tertiary boundary (northern Morocco): $\delta^{18}\text{O}$ record of phosphatic fish debris, *Palaeogeography, Palaeoclimatology, Palaeoecology*, **105**, 235–43.
- Lightfoot, E., and O'Connell, T. C., 2016, On the use of biomineral oxygen isotope data to identify human migrants in the archaeological record: intra-sample variation, statistical methods and geographical considerations, *PLoS One*, **11**(4), e0153850.
- Longinelli, A., 1984, Oxygen isotopes in mammal bone phosphate: a new tool for paleohydrological and paleoclimatological research? *Geochimica et Cosmochimica Acta*, **48**, 385–90.
- Marshall, J. D., Brooks, J. R., and Lajtha, K., 2007, Sources of variation in the stable isotopic composition of plants, in *Stable isotopes in ecology and environmental science* (eds. R. Michener and K. Lajtha), 22–60, Blackwell, Oxford.
- Mauder, M., Ntoutsis, E., Kröger, P., Grupe, G., Toncala, A., and Hölzl, S., 2016a, Applying data mining methods for the analysis of stable isotope data in bioarchaeology, in IEEE 12th International Conference on eScience, Baltimore, MD, USA, 23–27 October 2016.
- Mauder, M., Ntoutsis, E., Kröger, P., and Kriegel, H.-P., 2016b, Towards predicting places of origin from isotopic fingerprints: a case study on the mobility of people in the Central European Alps, in *Isotopic landscapes in bioarchaeology* (eds. G. Grupe and G. C. McGlynn), 221–33, Springer, Berlin.
- Mayr, C., Grupe, G., Lihl, C., and Toncala, A., 2016, Linking oxygen isotopes of animal-bone phosphate with altimetry—results from archaeological finds from a transect in the Alps, in *Isotopic landscapes in bioarchaeology* (eds. G. Grupe and G. C. McGlynn), 157–72, Springer, Berlin.
- Munro, L. E., Longstaffe, F. J., and White, C. D., 2008, Effects of heating on the carbon and oxygen-isotope compositions of structural carbonate in bioapatite from modern deer bone, *Palaeogeography, Palaeoclimatology, Palaeoecology*, **266**, 142–50.
- Park, G., 2014, *Die Geologie Europas*, Wissenschaftliche Buchgesellschaft, Darmstadt.
- Pellegrini, M., Pouncett, J., Jay, M., Pearson, M. P., and Richards, M. P., 2016, Tooth enamel oxygen 'isoscapes' show a high degree of human mobility in prehistoric Britain, *Science Reports*, **6**, 34986. <https://doi.org/10.1038/srep34986>.
- Piga, G., Santos-Cubedo, A., Moya Sola, S., Brunetti, A., Malgosa, A., and Enzo, S., 2009, An X-ray diffraction (XRD) and X-ray fluorescence (XRF) investigation in human and animal fossil bones from Holocene to Middle Triassic, *Journal of Archaeological Science*, **39**, 857–68.
- Pollard, A. M., Pellegrini, M., and Lee-Thorp, J., 2011, Technical Note: Some observations on the conversion of dental enamel $\delta^{18}\text{O}_p$ values to $\delta^{18}\text{O}_w$ to determine human mobility, *American Journal of Physical Anthropology*, **145**, 499–504.
- Price, T. D., Frei, R., Bäckström, Y., Frei, K. M., and Ingvarsson-Sundstrom, A., 2017, Origins of inhabitants from the 16th century Sala (Sweden) silver mine cemetery—a lead isotope perspective, *Journal of Archaeological Science*, **80**, 1–3.
- Rink, W. J., and Schwarcz, H. P., 1995, Test for diagenesis in tooth enamel: ESR dating signals and carbonate contents, *Journal of Archaeological Science*, **22**, 251–5.
- Rozanski, K., Araguás-Araguás, L., and Gonfiantini, R., 1992, Relation between long-term trends of oxygen-18 isotope composition of precipitate and climate, *Science*, **258**, 981–5.
- Rozanski, K., Araguás-Araguás, L., and Gonfiantini, R., 1993, Isotopic patterns in modern global precipitation, in *Climate change in continental isotopic records* (eds. P. K. Swart, K. C. Lohmann, J. McKenzie, and S. Savin), 1–37, Geophysical Monograph No. 78, American Geophysical Union, Washington D.C.
- Schmahl, W., Kocsis, B., Toncala, A., and Grupe, G., 2016, Mineralogic characterisation of archaeological bone, in *Isotopic landscapes in bioarchaeology* (eds. G. Grupe and G. C. McGlynn), 91–110, Springer, Berlin.
- Schmahl, W., Kocsis, B., Toncala, A., Wycisk, D., and Grupe, G., 2017, The crystalline state of archaeological bone material, in *Across the Alps in prehistory. Isotopic mapping of the Brenner Passage by bioarchaeology* (eds. G. Grupe, A. Grigat, and G. C. McGlynn), 75–104, Springer, Cham.
- Schürch, M., Kozel, R., Schotterer, U., and Trippet, J.-P., 2003, Observation of isotopes in the water cycle—the Swiss National Network (NISOT), *Environmental Geology*, **45**, 1–1.
- Shotyk, W., Weiss, D., Appleby, P. G., Cheburkin, A. K., Frei, R., Gloor, M., Kramers, J. D., Reese, S., and van der Knaap, W. O., 1998, History of atmospheric lead deposition since 12,370 ^{14}C yr BP from a peat bog, Jura Mountains, Switzerland, *Science*, **281**, 1635–40.

- Söllner, F., Toncala, A., Hölzl, S., and Grupe, G., 2016, Determination of geo-dependent bioavailable $^{87}\text{Sr}/^{86}\text{Sr}$ isotopic ratios for archaeological sites in the Inn Valley (Austria): a model calculation, in *Isotopic landscapes in bioarchaeology* (eds. G. Grupe and G. C. McGlynn), 123–40, Springer, Heidelberg.
- Stathopoulou, E. T., Psycharis, V., Chryssikos, G. D., Gionis, V., and Theodorou, G., 2008, Bone diagenesis: new data from infrared spectroscopy and X-ray diffraction, *Palaeogeography, Palaeoclimatology, Palaeoecology*, **266**, 168–74.
- Toncala, A., Söllner, F., Mayr, C., Hölzl, S., Heck, K., Wycisk, D., and Grupe, G., 2017, Isotopic map of the Inn–Eisack–Adige–Brenner Passage and its application to prehistoric human cremations, in *Across the Alps in prehistory—Isotopic mapping of the Brenner Passage by bioarchaeology* (eds. G. Grupe, A. Grigat, and G. C. McGlynn), 127–227, Springer, Cham.
- Turner, B. L., Kamenov, G. D., Kingston, J. D., and Armelagos, G. J., 2009, Insights into immigration and social class at Macchu Picchu, Peru based on oxygen, strontium, and lead isotopic analysis, *Journal of Archaeological Science*, **36**, 317–32.
- Vennemann, T. W., Fricke, H. C., Blake, R. E., O’Neil, J. R., and Colman, A., 2002, Oxygen isotope analysis of phosphates: a comparison of techniques for analysis of Ag_3PO_4 , *Chemical Geology*, **185**, 321–36.

SUPPORTING INFORMATION

Additional Supporting Information may be found online in the supporting information tab for this article.

Table S1 Sample description, geographical coordinates from north to south of the sites, and isotopic ratios

Table S2. Isotopic spacings between animal bones recovered from the same site

Figure S1. Spacings of $^{87}\text{Sr}/^{86}\text{Sr}$ isotopic ratios per site (see Tab. S2)

Figure S2. Pairwise plots of the first five components of the principal component analysis (PCA) (see Tab. 2)